

Cs nD_J Rydberg-atom macrodimers formed by long-range multipole interaction

Xiaoxuan Han^{1,2}, Suying Bai^{1,2}, Yuechun Jiao^{1,2}, Liping Hao^{1,2}, Yongmei

Xue^{1,2}, Jianming Zhao^{1,2,*}, Suotang Jia^{1,2}, and Georg Raithel^{1,3}

¹State Key Laboratory of Quantum Optics and Quantum Optics Devices,
Institute of Laser Spectroscopy, Shanxi University, Taiyuan 030006, China

²Collaborative Innovation Center of Extreme Optics, Shanxi University, Taiyuan 030006, China and

³Department of Physics, University of Michigan, Ann Arbor, Michigan 48109-1120, USA

Long-range macrodimers formed by D -state cesium Rydberg atoms are studied in experiments and in calculations. Cesium $62D_J$ - $62D_J$ Rydberg-atom macrodimers, bonded via long-range multipole interaction, are prepared by two-color photo-association in a cesium atom trap. The first color (pulse A) resonantly excites seed Rydberg atoms, while the second (pulse B, detuned by the molecular binding energy) resonantly excites the Rydberg-atom macrodimer states below the $62D_J$ pair asymptotes. The Rydberg-atom molecules are measured by extraction of auto-ionization products and Rydberg-atom electric-field ionization, and ion detection. Molecular spectra are compared with calculations of adiabatic molecular potentials. The lifetime of the molecules is obtained from exponential fits to the dependence of the molecular signal on the detection delay time; lifetimes of about $6 \mu\text{s}$ are found.

PACS numbers: 32.80.Ee, 33.20.-t, 34.20.Cf

Recently molecules involving one or more Rydberg excitations have attracted considerable attention due to their unusual properties, which include exotic adiabatic potentials, vibrational levels that reveal details of the binding potentials, and permanent dipole moments. Two kinds of Rydberg molecules with distinct binding mechanisms have been observed, Rydberg-ground molecules and Rydberg-Rydberg macrodimers. Rydberg-ground molecules, consisting of a Rydberg electron and a ground-state atom and formed with a low-energy scattering mechanism, have been theoretically predicted [1, 2] and experimentally observed for Rydberg S -states [3, 4], P -states [5], and D -states [6, 7], and for high-angular-momentum states [8–12]. Molecules consisting of two Rydberg atoms that are bound by long-range dipolar and higher-order multipole interactions have been predicted [13] and observed in an ultracold gas [14–16]. These Rydberg-Rydberg molecules are macrodimers, as their bond lengths are $\sim 4n^2$ and can easily exceed $1 \mu\text{m}$. Since the bond length generally exceeds the LeRoy radius, the exchange interaction is negligible. Deiglmayr *et al.* have prepared pair states of Cs near the $nsn'f$ and $npnp$ asymptotes for $22 \leq n \leq 32$ [15], and $43p44s$ [16] macrodimer molecules bounded by long-range dipolar interaction.

Here we report on the observation of Cs macrodimers of the type $2 \times 62D_J$ on the red-detuned side of the $62D_J$ atomic resonance. We excite the molecules via two-step, two-color photoassociation using two laser pulses at $\approx 510 \text{ nm}$ whose frequencies differ by the binding energy of the molecule, as sketched in Fig. 1(a). A small number of seed Rydberg atoms, denoted as A-atoms, is resonantly excited from the ground state using a laser-pulse pair labeled A. The A-pulses are two-photon resonant with the

interaction-free Rydberg level energy $|r\rangle = 62D_J$ (see Fig. 1(a)). The detuning from the intermediate $6P_{3/2}$ -state is 220 MHz. The 510-nm component of the second laser pulse pair, labeled B, is detuned relative to that of the pulse pair A by an amount equal to the molecular binding energy. The 852-nm components of pulse pairs A and B have the same frequency. The B-pulses excite Rydberg atoms that are close to the already existing seed atoms (A-atoms), at a distance at which stable, deeply bound Rydberg molecules are generated. Owing to the doubly-resonant character of two-color photoassociation, the excitation rate is greatly enhanced in comparison with that of single-color photoassociation.

The Rydberg-atom macrodimer experiment is performed in a Cs magneto-optical trap (MOT) with temperature $\sim 100 \mu\text{K}$, see Fig. 1(b). After switching off the MOT beams, we turn on the photoassociation pulses A and B (the MOT magnetic field is always on). The lower-transition laser (852 nm, Topptica DLpro, $\sim 100 \text{ kHz}$ linewidth) is stabilized to the $|6S_{1/2}, F=4\rangle (|g\rangle) \rightarrow |6P_{3/2}, F'=5\rangle (|e\rangle)$ transition using polarization spectroscopy [17], and tuned using a double-pass acousto-optic modulator (AOM). The upper-transition laser (510 nm, Topptica TA SHG110, 1 MHz linewidth) is stabilized to excite $62D_J$ Rydberg atoms using a Rydberg EIT reference signal obtained from a Cs room-temperature vapor cell [18], and double-passed through another AOM. For the pulse pair A, the 510-nm AOM frequency is set to resonantly excite Rydberg-A seed atoms. The 510-nm AOM frequency is scanned to resonantly photo-associate the B-atoms to the already present A-atoms to form a molecule, as sketched in Fig. 1(b). During the scan, the B-pulse laser power is held fixed using a PID [18] feedback loop that controls the RF power supplied to the 510-nm AOM. The 852-nm laser has a power of $\sim 220 \mu\text{W}$ and Gaussian waist of $\omega_{852} \approx 80 \mu\text{m}$. The 510-nm beam has a maximum power of

* Corresponding author: zhaojm@sxu.edu.cn

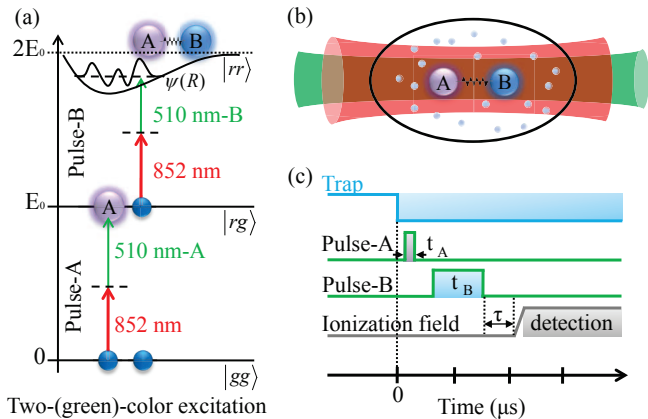


FIG. 1. Level diagram and sketch of a vibrational wavefunction (a) and schematic of the experiment (b) for two-color double-resonant excitation of $2 \times 62D_J$ Rydberg-atom macrodimers. The 852 nm and 510 nm Rydberg excitation beams counterpropagate through a cold Cs atom cloud. The pulse pair A is tuned into two-photon resonance to prepare the seed Rydberg atoms (atom A). To study Rydberg-atom macrodimers, the frequency of the 510-nm component of the pulse pair B is scanned over a range of ± 70 MHz relative to the atomic resonance. (c) Timing sequence. After switching off the MOT beams, we sequentially apply the A-pulses and B-pulses. Rydberg atoms and molecular signals are detected via ion extraction or electric-field ionization. An optional wait time $\tau \lesssim 40 \mu\text{s}$ between the B-pulses and the ion extraction ramp allows us to study the decay / autoionization behavior of the Rydberg atoms and molecules.

10 mW with a waist $\omega_{510} \simeq 40 \mu\text{m}$ in MOT center, and its power is controlled using neutral attenuators. The timing diagram is shown in Fig. 1(c). To minimize the effect of stray electric fields on atomic and molecular spectra, three pairs of electrodes are placed around the excitation region to compensate the stray electric field. The residual field at the MOT center is less than 25 mV/cm, as found by Stark spectroscopy of the $60D_J$ Rydberg states. After excitation, Rydberg atoms and molecules are detected using the electric-field ionization method (ionization ramp rise time $3 \mu\text{s}$), while ions formed by Penning ionization of Rydberg atoms or molecules are extracted with a smaller electric field. The extracted ions are detected with a microchannel plate (MCP) detector. Spontaneously formed ions and field-ionized Rydberg atoms are discriminated by their time of flight to the detector (timing see Fig. 1(c)). Three potential grids are arranged along the path of the ions to the MCP, forming an ion lens that is used to collimate the ions onto the MCP and to thereby increase the ion collection efficiency. We have used Simion to simulate the ion trajectories and to optimize the ion lens. Voltages of 0, 63 and 0 V, applied in this order to the three grids, yield maximum signal strength under our experimental conditions.

Figure 2(a) shows calculated adiabatic potentials be-

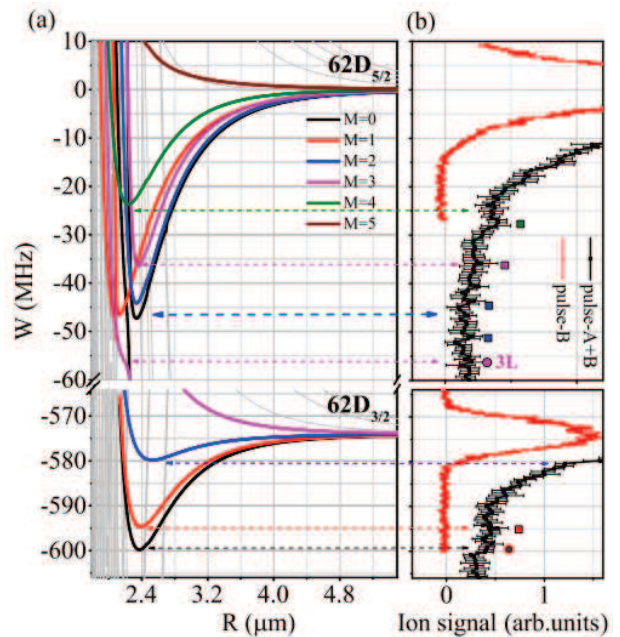


FIG. 2. (a) Calculations of adiabatic potential curves for cesium Rydberg pair states, $2 \times 62D_J$, with $M=0$ (light gray) and Rydberg-atom macrodimer potentials with the indicated M -values. (b) Spectra measured with single-color excitation (pulse-B only; red lines) and $2 \times 62D_J$ macrodimer spectra for two-color excitation (pulses A and B; black lines). The one-color spectra mark the $2 \times 62D_J$ asymptotes (detuning $W = 0$); they are absent of any significant molecular signal. Horizontal dashed lines indicate the minima of the $2 \times 62D_J$ molecular potentials.

low the Cs_2 ($62D_J$ - $62D_J$) asymptote for the relevant values of the projection of the total electronic angular momentum of the Rydberg molecules, M . For given J , the allowed values are $|M| = 0, 1, \dots, 2J$. Details of the calculation are explained below. All values of M support binding potentials, except the maximal values, $|M| = 2J$. The binding potentials exhibit minima that are up to ~ 50 MHz deep, at distances of $\sim 2.4 \mu\text{m}$. The figure also shows light-gray potentials for $M = 0$ that have very narrow anti-crossings with the binding potentials. The macrodimer molecular states on the binding potentials are expected to produce signatures in the excitation rates in our double-resonance spectroscopy experiment. In particular, the lowest vibrational states or resonances are expected to produce local maxima in oscillator strength in the vicinity of the calculated potential-energy minima of the binding potentials.

The black line in the upper panel of Fig. 2(b) shows the two-color photoassociation spectrum recorded below the $2 \times 62D_{5/2}$ asymptote. The 852-nm and 510-nm beam powers are $210 \mu\text{W}$ and 1.2 mW , respectively. The duration of the A-pulses is $0.2 \mu\text{s}$, and that of the B-pulses $5.0 \mu\text{s}$. Rydberg atoms and molecules are field-ionized and detected immediately after the B-pulses. Comparing the two spectra, it becomes immediately obvious that

at detunings $|W| \gtrsim 10$ MHz the B -pulses only generate signal when the A -pulses are on, *i. e.* if the sample is seeded with Rydberg atoms (A -atoms). The fact that the B -pulses fail to produce any signal at detunings $|W| \gtrsim 10$ MHz, unless the 25-times shorter seed pulses are present, demonstrates efficient doubly-resonant photoassociation at large detunings. The bottom panel of Fig. 2(b) shows analogous spectra for $2 \times 62D_{3/2}$ Rydberg-atom macrodimers. Due to the smaller transition matrix element of the $62D_{3/2}$ level, for $J = 3/2$ we use an A pulse duration of $0.4 \mu\text{s}$; the duration of the B -pulses is the same as in the $J = 5/2$ -case.

The measured photo-association signal consists of a structure-less part that rapidly drops as a function of detuning. This part of the signal is attributed to van-der-Waals-type interaction at distances and conditions away from the aforementioned potential minima. The two-color photo-association spectra for $J = 5/2$ (top panel in Fig. 2(b)) demonstrate additional peaks near the minima of the highlighted adiabatic potentials, marked with squares. The peak at detuning -56 MHz, marked with a red-filled circle and labeled 3L, is attributed to an avoided crossing of adiabatic potentials that belong to $M = 3$. The anti-crossing generates a near-stationary region over which the adiabatic potential surface is flat, resulting in an enhanced spectroscopic response.

In the two-color photo-association spectra for $J = 3/2$ (bottom panel in Fig. 2(b)) we also clearly see peaks, on top of the van-der-Waals background, that arise from binding adiabatic potentials. The peaks in the measured molecular signal occur at detunings of -20 and -25 MHz relative to the $2 \times 62D_{3/2}$ -asymptote. These spectra result from $M = 0$ and 1, marked with a red square and a gray circle, respectively. The spectrum in the bottom panel of Fig. 2(b) does not show a peak -6 MHz, the binding energy predicted for the $M = 2$ -case. The absence of this peak may be due to the small size of the binding and the proximity to the atomic background signal (red measured curve).

To model the molecules, we consider the multipole interaction, V_{int} , in the product space of two Rydberg atoms labeled A and B [15, 19],

$$\begin{aligned} \hat{V}_{int} &= \sum_{L_A=1}^{L_{maxA}} \sum_{L_B=1}^{L_{maxB}} \sum_{\Omega=-L_{<}}^{L_{<}} \frac{(-1)^{L_B} f_{AB\Omega}}{R^{L_A+L_B+1}} Q_A(\hat{\mathbf{r}}_A) Q_B(\hat{\mathbf{r}}_B) \\ Q_X(\hat{\mathbf{r}}_X) &= \sqrt{\frac{4\pi}{2L_X+1}} \hat{r}_X^{L_X} Y_{L_X}^{\Omega}(\hat{\mathbf{r}}_X) \quad , \quad X = A, B \\ f_{AB\Omega} &= \frac{(L_A+L_B)!}{\sqrt{(L_A+\Omega)!(L_A-\Omega)!(L_B+\Omega)!(L_B-\Omega)!}} \end{aligned} \quad (1)$$

where L_A and L_B are the multipole orders of atoms A and B , and $L_{<}$ is the lesser of L_A and L_B . The sums over L_A and L_B start at 1, because the atoms have no monopole moment, and are truncated at maximal orders L_{maxA} and L_{maxB} . Here we set

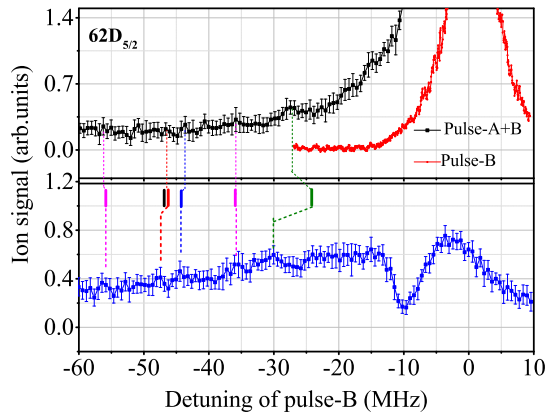


FIG. 3. Measured spectra of $2 \times 62D_{5/2}$ macrodimers for field ionization detection with $0\text{-}\mu\text{s}$ delay (upper panel) and for ion extraction detection with $10\text{-}\mu\text{s}$ delay (lower panel). The vertical lines denote the calculated positions of the bonding energy.

$L_{maxA}=L_{maxB}=2$; the calculation then includes dipole-dipole, dipole-quadrupole and quadrupole-quadrupole interactions. The factor $f_{AB\Omega}$ depends on L_A , L_B and the counting index Ω under the third sum. The single-atom operators $\hat{\mathbf{r}}_A$ and $\hat{\mathbf{r}}_B$ are the radial positions of the Rydberg electrons in atoms A and B . The operators Q include radial matrix elements, such as $\hat{r}_A^{L_A}$, and spherical harmonics that depend on the angular parts of the Rydberg-electron positions, such as $Y_{L_A}^{\Omega}(\hat{\mathbf{r}}_A)$.

We diagonalize the Hamiltonian of the Rydberg-atom pair on a dense grid of the internuclear separation, R . Due to global azimuthal symmetry, the projection of the sum of the electronic angular momenta, $M = m_{jA} + m_{jB}$, is conserved. Numerically calculated potential curves are shown in Fig. 2(a) for Cs Rydberg-atom pair states $2 \times 62D_J$, for values of M indicated by different colors. Most adiabatic potentials do not exhibit minima that could support bound macrodimer states. Those potentials, shown in light gray for the case $M = 0$, are mostly confined to the domain $R \lesssim 2.3 \mu\text{m}$. Several of them exhibit unresolved (narrow) intersections with the adiabatic potential curves that do have minima which should support macrodimer states. Since the crossings are very narrow (below the vibrational periods of the macrodimer states), we expect that they should not destroy spectral signatures of those states. The crossings may reduce the lifetimes of the macrodimer states; this topic may be addressed in future work.

The calculated potential-energy minima represent stationary points of the energy as a function of the internuclear position, and are expected to yield signal maxima indicative of metastable Rydberg-atom molecules. In Fig. 2 these are denoted by horizontal dashed lines for the various M . Note the $M = 0, 1, 2$ potential minima are so close to each other that we do not expect to resolve their spectroscopic signatures in the current experiment. The cases $M = 3$ and $M = 4$ should produce separate peaks at lesser binding energies. For comparison, in table we

TABLE I. The calculated and measured binding energy of the potential of cesium $62D_{5/2}$ - $62D_{5/2}$ for a quantum number M in MHz.

$M =$	0	1	2	3	4	3L
$62D_{5/2}$ theo.	-47	-46	-44	-36	-24	-55
exp.		-46.6	-43.6	-35.8	-27.4	-56.3
$62D_{3/2}$ theo.	-25	-20	-6	-	-	-
exp.	-25.5	-20.3	-	-	-	-

list the calculated potential minima (bonding energies) and the energies of measured peaks in the molecular spectra. From Fig. 2 and Table. 1, we see that the calculations of the binding energies of $2 \times 62D_J$ Rydberg dimers are consistent with the measured molecular spectra.

The potentials for $M=3$, indicated with purple curves in Fig. 2(a), include a potential that exhibits an isolated potential minimum for Rydberg-atom macrodimers, at a binding energy of -36 MHz. This $M = 3$ adiabatic potential also anti-crosses with a different, lower-lying $M = 3$ -potential. The anti-crossing leads to a knee point on the lower $M = 3$ -potential, denoted 3L in Fig. 2(b).

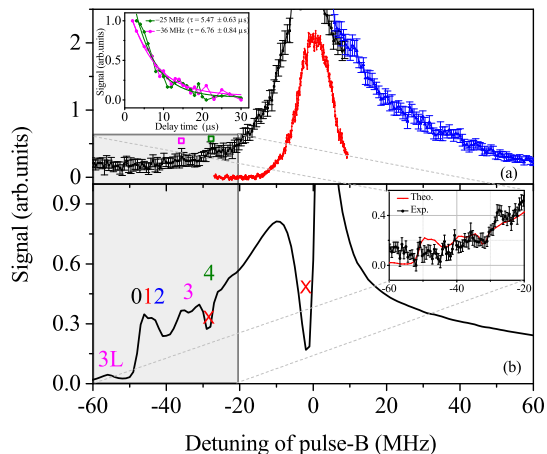


FIG. 4. Measured spectra (a) and calculation for atom density 10^8 cm^{-3} (b) for double-resonant photo-association of $62D_{5/2}$ atom pairs vs pulse-B detuning. The dips marked with red crosses are artifacts in the calculation, caused by the finite step size and range of the internuclear separation, and narrow crossings between uncoupled or weakly coupled adiabatic potentials. Inset (a): Normalized signal as a function of delay time, τ in Fig. 1(c) for pulse-B detunings that correspond to the bond energy of the $M = 3$ and $M = 4$ adiabatic potentials (-36 MHz and -25 MHz, marked with squares in (a)), together with exponential fits (solid lines). Inset (b): Zoom-in of experimental and calculated spectra for pulse-B detuning between -60 and -20 MHz.

Rydberg macrodimers are likely to undergo auto-ionization (or, Penning ionization out of a bound Rydberg-Rydberg state) [20, 21] due to the proximity of the constituents. This allows for detection of Rydberg-atom macrodimers via ion extraction, leading to a signal with a greatly reduced single-atom background (the

atomic signal in Fig. 2). In this method, after photoassociation we insert a wait time, $\tau = 10 \mu\text{s}$, during which the Rydberg molecules may undergo Penning ionization. We then apply an electric field that is less than the ionization field for the selected atomic state; the electric field is, however, sufficient to collect any spontaneously formed ions onto the MCP. In the bottom curve in Fig. 3 we show a spectrum of Rydberg-atom molecules obtained with the ion extraction method, below the $2 \times 62D_{5/2}$ asymptote. For comparison, in the top curve we display the analogous signal obtained with the field-ionization method. The short vertical lines indicate the bonding energy positions deduced from the calculations of adiabatic potentials. We note that the strength of the molecular signal is very similar in both cases, i.e. almost all Rydberg molecules Penning-ionize during the waiting time. Close to the atomic resonance, the ion extraction signal is cleaner, as the spectroscopic signatures are less obscured by the atomic signal. Close to the atomic resonance we find a pronounced, broad dispersive structure in the on extraction signal, characterized mostly by a marked absence of extracted ions at ~ -10 MHz. This may indicate a reduced auto-ionization rate of vibrationally excited Rydberg molecules, caused by a more diabatic behavior close to intersections with ionizing adiabatic potentials. The spectral structure at ~ -10 MHz will be investigated in more detail in future work.

The model outlined above also yields the two-body excitation rate of two-color photo-association of the binary molecules. The calculated rates are averaged over a random distribution of the angle between internuclear axis and laboratory frame (defined by laser polarizations), and summed over M ($M = -5, -4, \dots, 5$). Figure 4 shows measured (a) and calculated (b) two-color excitation spectra of $62D_{5/2}$ - $62D_{5/2}$ pairs. On the red-detuned side, the structures in the calculated and measured spectra, indicative of the production of macrodimer Rydberg molecules, are in reasonable agreement. This is seen in the inset of Fig. 4(b), where we compare measured and calculated spectra in the pulse-B detuning range -20 to -60 MHz. Several adiabatic potentials exhibit minima in that range. On the blue-detuned side, both the measured and calculated spectra demonstrate excitation of $62D_{5/2}$ - $62D_{5/2}$ pairs on repulsive van der Waals adiabatic potentials. Those dimers dissociate very quickly.

To investigate the lifetime of Rydberg-atom macrodimers, the pulse-B detuning is kept fixed at bonding energies of -25 and -36 MHz. After some interaction time (delay time τ in Fig. 1(c)), we apply a ramped electric field to separately measure the signal fractions due to ions that result from auto-ionization of the molecules and due to Rydberg molecules that have not ionized. In the inset in Fig. 4(a), we show the (non-ionized) molecular signals as a function of τ and exponential fits (solid lines). The respective fitted decay times, $5.5 \pm 0.7 \mu\text{s}$ and $6.8 \pm 0.9 \mu\text{s}$, provide an initial indication for the lifetimes of the $2 \times 62D_{5/2}$ Rydberg macrodimers.

In conclusion, we have studied long-range Rydberg-atom macrodimers using a two-color photo-association method, in which the first color resonantly excites seed Rydberg atoms, while the second color resonantly photo-associates Rydberg atoms to the seed atoms. The frequency difference between the two colors yields the molecular bonding energy. We have detected the molecules via Rydberg-atom electric field ionization and, alternatively, by time-delayed ion extraction detection that result from auto-ionization of the molecules. The spectra show reasonable agreement with calculated molecular adiabatic potentials. In the future, one may study mixed-parity photo-association schemes, realized by simultaneous two-photon and three-photon Rydberg-atom excitation. Also, a detailed understanding of the lifetime reduction of the D -state Rydberg-atom

molecules, caused by interaction with unbound adiabatic potentials, will require further study. Also, it has been suggested that Rydberg-atom macrodimers can be used to study vacuum fluctuations [22, 23], to quench ultracold collisions [13], and to measure correlations in quantum gases [14, 24].

The work was supported by the National Key R&D Program of China (Grant No. 2017YFA0304203), the National Natural Science Foundation of China (Grants No. 11274209, 61475090, 61675123), Changjiang Scholars and Innovative Research Team in University of Ministry of Education of China (Grant No. IRT13076), and the State Key Program of National Natural Science of China (Grant No. 11434007). GR acknowledges support by the National Science Foundation (PHY-1506093) and BAIREN plan of Shanxi province.

-
- [1] C. H. Greene, A. S. Dickinson, and H. R. Sadeghpour, Phys. Rev. Lett. **85**, 2458 (2000).
- [2] I. Lesanovsky, P. Schmelcher, and H. R. Sadeghpour, J. Phys. B **39**, L69 (2006).
- [3] V. Bendkowsky, B. Butscher, J. Nipper, J. P. Shaffer, R. Löw, and T. Pfau, Nature **458**, 1005 (2009).
- [4] V. Bendkowsky, B. Butscher, J. Nipper, J. B. Balewski, J. P. Shaffer, R. Löw, T. Pfau, W. Li, J. Stanojevic, T. Pohl, and J. M. Rost, Phys. Rev. Lett. **105**, 163201 (2010).
- [5] M. A. Bellos, R. Carollo, J. Banerjee, E. E. Eyler, P. L. Gould, and W. C. Stwalley, Phys. Rev. Lett. **111**, 053001 (2013).
- [6] D. A. Anderson, S. A. Miller, and G. Raithel, Phys. Rev. Lett. **112**, 163201 (2014).
- [7] A. T. Krupp, A. Gaj, J. B. Balewski, P. Ilzhöfer, S. Hofferberth, R. Löw, T. Pfau, M. Kurz, and P. Schmelcher, Phys. Rev. Lett. **112**, 143008 (2014).
- [8] J. Tallant, S. T. Rittenhouse, D. Booth, H. R. Sadeghpour, and J. P. Shaffer, Phys. Rev. Lett. **109**, 173202 (2012).
- [9] T. Niederprüm, O. Thomas, T. Eichert, H. Ott, Phys. Rev. Lett. **117**, 123002 (2016).
- [10] K. S. Kleinbach, F. Meinert, F. Engel, W. J. Kwon, R. Löw, T. Pfau and G. Raithel, Phys. Rev. Lett. **118**, 223001 (2017).
- [11] D. Booth, S. T. Rittenhouse, J. Yang, H. R. Sadeghpour and J. P. Shaffer, Science **348**, 6230 (2015).
- [12] T. Niederprüm, O. Thomas, T. Eichert, C. Lippe, J. PérezRíos, C. H. Greene and H. Ott, Nat. Commun. **7**, 12820 (2016).
- [13] C. Boisseau, I. Simbotin, and R. Côté, Phys. Rev. Lett. **88**, 133004 (2002).
- [14] K. R. Overstreet, A. Schwettmann, J. Tallant, D. Booth and J. P. Shaffer, Nature **5**, 581 (2009).
- [15] J. Deiglmayr, H. Saßmannshausen, P. Pillet, and F. J. Merkt, Phys. Rev. Lett. **113**, 193001 (2014).
- [16] H. Saßmannshausen, and J. Deiglmayr, Phys. Rev. Lett. **117**, 083401 (2016).
- [17] C. P. Pearman, C. S. Adams, S. G. Cox, P. F. Griffin, D. A. Smith, and I. G. Hughes, J. Phys. B **35**, 5141 (2002).
- [18] Y. Jiao, J. K. Li, L. M. Wang, H. Zhang, J. M. Zhao, and S. T. Jia, Chin. Phys. B **25** 053201 (2016).
- [19] A. Schwettmann, J. Crawford, K. R. Overstreet, and J. P. Shaffer, Phys. Rev. A **74**, 20701 (2006).
- [20] M. Viteau, A. Chotia, D. Comparat, D. A. Tate, T. F. Gallagher, and P. Pillet, Phys. Rev. A **78**, 040704 (2008).
- [21] H. Saßmannshausen, F. Merkt, and J. Deiglmayr, Phys. Rev. A **92**, 032505 (2015).
- [22] L. H. Ford, and T. A. Roman, Ann. Phys. **326** 2294 (2011).
- [23] G. Menezes, and N. F. Svaiter, Phys. Rev. A **92**, 062131 (2015).
- [24] M. Stecker, H. Schefzyk, J. Fortágh, and A. Günther, New J. Phys. **19**, 043020 (2017).